18th Brazilian Congress of Thermal Sciences and Engineering
November 16-20, 2020 (Online)

ENC-2020-0056
ANALYSIS IN DYNAMOMETER OF THE PERFORMANCE AND EMISSIONS OF A SMALL DIESEL CYCLE ENGINE OPERATING WITH ETHANOL - CASTOR OIL BLENDS

Maicon Douglas Bernardi
Carlos Roberto Altafini
Universidade de Caxias do Sul, Caxias do Sul, Brazil
e-mails: maicondbernardi@gmail.com; craltafini@ucs.br.

Giovani Dambros Telli
Universidade Federal do Rio Grande do Sul, Postgraduate Program in Mechanical Engineering, PROMEC, Porto Alegre, Brazil
e-mail: giovani.telli@gmail.com.

Abstract. *The purpose of this article is to investigate the operation of a compression ignition engine operating with hydrous ethanol (HET) and castor oil (OM) blends, in two volume concentrations: 60% HET and 40% OM and 70% HET and 30% OM. The experiments were conducted with a single cylinder engine coupled to a dynamometer at full load, varying its speed, the compression ratio (20:1 and 21.5:1) and start of injection (10° and 17°, before top dead center - BTDC). In general, the results indicated that the torque and, consequently, the power, developed by the engine with diesel fuel (DO) was higher than HET-OM blends, with lower specific fuel consumption. Fuel conversion efficiencies of blends was higher than that of DO. The results indicated a significant reduction in the exhaust gas temperature in operation with HET-OM blends. The emissions of CO, CO_2 and NO_x obtained with the blends decreased compared to those obtained with the DO operation. Moreover, the smoke index significantly reduced in the operation with HET-OM blends. The HC emission for blends were higher than that of DO. In general, the results obtained were satisfactory, demonstrating that HET-OM blends can be used in diesel cycle engines, under certain conditions, resulting in emission reductions and higher fuel conversion efficiency.*

Keywords: *compression ignition engine, ethanol-castor oil blends, dynamometer, performance and emissions parameters.*

1. INTRODUCTION

Currently, fuels used in vehicles and stationary engines are easily found at filling stations, having, in general, renewable fuels diluted in them, which have been inserted in greater proportions over the years. In this regard, according to the International Energy Agency (2018), the production of biofuels has been increasing over the years, Latin America and Asia have the highest growth in the production of biofuels.

In recent years, various researchers have carried out investigations about the performance of diesel cycle engines operating with biofuels. According to Telli et al. (2018), the use of renewable fuels, such as vegetable oils in CI engines is an alternative way to reduce pollutant emissions and our dependence on diesel fuel. The reason is mainly that these fuels are produced from renewable raw material, which is an oxygenated, non-toxic, sulfur-free and biodegradable. Brunelli (2009) evaluated three types of biodiesel and found that the smoke index decreased in relation to that of diesel oil.

Prakash et al. (2018) evaluated the performance and emissions characteristics of a single cylinder, compression ignition engine operating on pure diesel fuel and pure castor oil. Moreover, the authors also studied three blends of diesel fuel, castor oil and bioethanol (BE) in different proportions. At full load, the results showed that the exhaust gas temperature increased when the engine operated with pure castor oil, about 8.5%. However, when the BE was used in the blends the exhaust gas temperature decreased. In addition, at full load, the specific NOx emission was 5.21 g/kWh for pure castor oil and 8.17 g/kWh for diesel fuel. The CO emissions from castor oil were higher than diesel fuel. The HC emissions from castor oil generated higher amounts of HC compared to diesel fuel. However, the HC emissions from the blends were lower than pure castor oil but still higher than pure diesel fuel.

Pinzi et al. (2018) studied the properties of mixtures of castor oil, hydrous ethanol and diesel fuel, the authors prepared and analyzed 16 samples with different concentrations. The authors observed that OM increases the solubility and stability of the mixtures. They also noted that the presence of ethanol reduces the viscosity of the mixture. Pinzi et

al. (2018) with a deep analysis conclude that the best mixture to meet the needs of application in compression ignition engines is OM30-ETH41.4-DO28.6. This ideal mixture met most of the limits set out by DIN EN 590, which is a suitable mixture for automotive and power generation applications. However, due to water content in ethanol, they recommended adjustments to the injection configuration and higher compression ratio.

Vailatti et al. (2016) studied a single-cylinder compression ignition engine, operating on dual fuel mode using ternary DO-HET-OM mixtures. The percentages of DO substitution ratio varied from 10% to 50% (in vol.). Experimental tests were also conducted with 100% replacement of DO by mixtures of HET-OM and in this mode of operation the samples were composed of 90%, 80% and 75% by volume of HET and the rest by OM. In HET-OM blends there was a 96% reduction in the opacity, exhaust gas temperatures decreased by 17.6%, fuel consumption increased by 52.4% and the engine's thermal efficiency decreased by almost 1.7%.

Due to the employability of biofuels and mainly to environmental factors, related to pollutant emissions by internal combustion engines, the study involved in this article aims to contribute with technical information on performance and emissions of a diesel engine operating with controlled mixtures of hydrated ethanol and castor oil with different compression rates and starts of injection.

2. EXPERIMENTAL PROCEDURE

Figure 1 schematically illustrates the experimental arrangement that was set up to perform the tests. The engine used in the experiments was Agrale, model M93, single cylinder, direct injection and its characteristics are presented in Table 1.

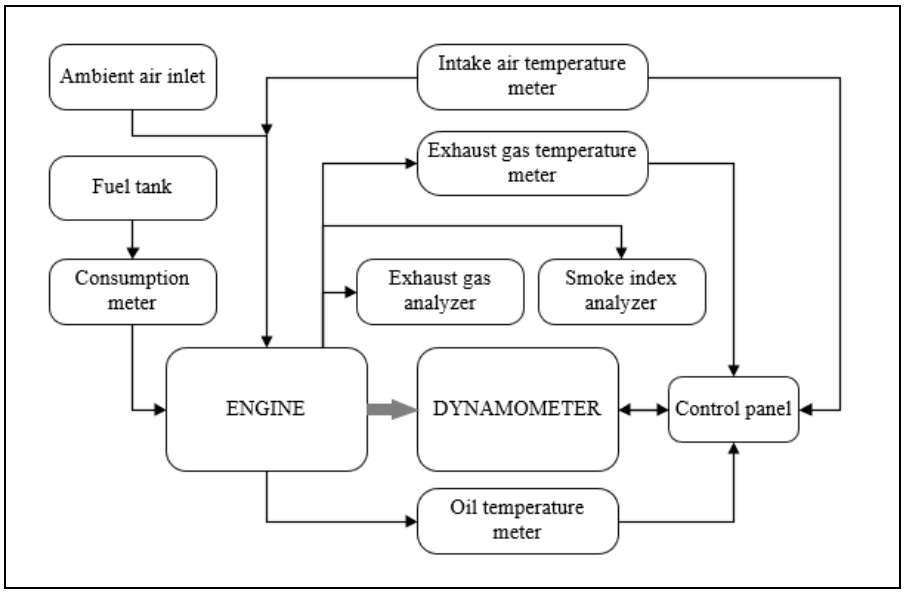

Figure 1. Experimental Scheme

Table 1. Main characteristics of the engine Agrale M93

Characteristics	Specification
Cycle	Diesel 4-stroke
Power at 2750 rpm	10.8 kW (14.7 cv)
Bore x stroke	90 x 105 mm
Volumetric displacement	668 cm³
Compression rate (CR)	20.0:1
Injection system	Bosch direct
Start of injection (SOI)	17° BTDC
Injection pressure	From 180 to 188 bar
Specific fuel consumption	240 g/kWh at 2100 rpm
Cooling	Air cooled

The engine was evaluated operating with DO (S10 – up to 10 ppm of sulphur) and with two HET-OM blends, in different volume proportions: 60% HET and 40% OM; and 70% HET and 30% OM; characterized as HET60-OM40 and HET70-OM30, respectively.

In the experiments was used an electric dynamometer, eddy currents of the Schenck brand, model W130-130 kW. The dynamometer has an electronic data acquisition system with an uncertainty measurement speed of ± 10 rpm. From the center of the dynamometer, a lever arm with a length of 0.310 m, having at its end a KRATOS load cell, model KCC, with a force capacity of 490 N and an approximate uncertainty of <0.2%. The load cell is responsible for measuring the load imposed by the dynamometer in the engine braking process. The heat generated by the dynamometer in the engine's braking process is dissipated by a water-cooling system. The dynamometer has a supervisory to control and monitor its operation and the engine, varying and monitoring the load imposed, rotation, torque and, consequently, power. In addition, the supervisory allows the visualization of several temperature measurements.

Fuel consumption was measured by weighing the fuel. A reservoir with a volumetric capacity of 20 liters was filled with fuel, with an upper part of it open to the atmosphere. The reservoir was connected to the engine's injection pump by means of an 8 mm internal diameter pipe. The reservoir was suspended above the engine by a load cell of the HBM brand, model U2B, with a force capacity of 980 N and an approximate uncertainty of <0.2%. The load cell was connected to a data acquisition equipment of the brand HBM, model Quantum MX840A, which was controlled using the software Catman Easy - AP 3.5. During the operation of the engine under different load conditions, for a period, the mass of the fuel was acquired. The mass variation resulting from the measurement interval served to determine the mass flow of fuel, according to Equation (1).

$$\dot{m}_c = \frac{m_i - m_f}{t} \cdot 3600 \tag{1}$$

where, $\dot{m}_c$ is the fuel mass flow rate [g/s], m_i is the initial mass of fuel [g], m_f is the final mass of fuel [g], and t is the measurement time [s].

Smoke index was determined by a Smoke Meter AVL, model 409D2, which has a measurement range of 0.0 to 9.0 UB (Bosch Unit; SZ-Bosch). The equipment resolution is 0.1 with a measurement uncertainty of 2% for the measurement range from 0.6 to 5.0 SZ-Bosch, without temperature variation, which can be from 0 to 50 °C. The equipment has a duct, which interconnects the exhaust system through which the engine's exhaust gases circulate, with its measuring device. A pump disposed inside the equipment causes an exhaust gas sample to be directed to a paper filter, which darkens with the passage of the gas sample. The device directs a light beam at the darkened paper and reads the smoke index according to the reflectance of the light by the paper, which can be viewed in an analogical way on the equipment's display.

An AVL gas analyzer, model DiCom 4000, was used to determine the gaseous emissions. The determination of O_2 and NO concentrations occurs by electrochemical sensors, whereas for HC, CO and CO_2, the measurement is performed by detecting the length in the infrared spectrum. The operating temperature is from 1 to 50 °C, with a maximum humidity of 90%. The measurement ranges, as well as their resolution, are reported in Table 2. In the tests, the measurement of CO, CO_2, HC and NO_x was performed.

Table 2. Specifications of the AVL gas analyzer DiCom 4000

Gas	Measurement range	Resolution
O_2	0 – 4%	0.01%
NO/NO_x	0 - 4000 ppm	1 ppm
HC	0 – 20000 ppm	1 ppm
CO	0 – 10%	0.01%
CO_2	0 – 20%	0.1%

Fluctuation densimeters Incoterm were used to measure the specific mass of the fuels in the ranges: 0.700 to 0.750 g/mL; 0.750 to 0.800 g/mL; 0.800 to 0.850 g/mL; 0.850 to 0.900 g/mL; 0.900 to 0.950 g/mL; and 0.950 to 1,000 g/mL. Viscosity measurements of fuels and mixtures were performed using an Anton Paar rheometer, physica model mcr 301, with cone-plate geometry. To measure the Higher Heating Value (*HHV*) of the DO, HET and OM, an Isoperibol calorimeter was used and followed the ASTM standard D4809-13 (Standard Test Method for Heat of Combustion of Liquid Hydrocarbon Fuels by Bomb Calorimeter - Precision Method).

For the measurement of the ambient parameters, a meteorological mini station Kestrel, model 4000, was used. These parameters were used to correct the performance parameters of the engine according to NBR ISO 1585 Standard. This mini station incorporates a barometer, with a range of 10 to 1100 mbar operation, 0.1 mbar resolution and measurement

uncertainty of ± 1.5 mbar. It also has the measurement of relative humidity, with an operating range from 0 to 100%, resolution of 0.1% and uncertainty of ± 3%.

From power, fuel consumption and the fuel Lower Heating Value measurements, the fuel conversion efficiency (η_f) was determined by Equation (2).

$$\eta_f = \frac{P}{\dot{m}_c \cdot LHV} \tag{2}$$

where P is the power produced [kW] and LHV_f is the Lower Heating Value of the fuel (DO or HET-OM blend) [kJ/kg]. The LHV_f was calculated from the DO, HET and OM *HHV* through Equation (3).

$$LHV = HHV - 2440 \cdot (9H + u) \tag{3}$$

where, H is the concentration of hydrogen in the fuel [%m] and u is the moisture concentration of the fuel [%m]. From the DO, HET and OM *LHV* known, the LHV_{fb} of the fuel blends can be obtained from Equation (4).

$$LHV_{fb} = y_{HET} \cdot LHV_{HET} + y_{OM} \cdot LHV_{OM} \tag{4}$$

where y_{HET} is the is the mass fraction of HET in the mixture, LHV_{HET} is the lower heating value of the HET [kJ/kg], y_{OM} is the mass fraction of OM in the mixture and LHV_{OM} is the lower heating value of the OM [kJ/kg].

To carry out the experiments, the procedures mentioned below were followed. The engine was started at idle, operating only with pure DO. After starting, the engine was subjected to a maximum free speed of 2950 rpm and through the dynamometer, a sufficient load was imposed to reach the maximum engine power. Thus, the engine ran for a sufficient period until the lubricating oil temperature stabilized.

When the temperature of the lubricating oil stabilized, the test started at the maximum power speed (2750 rpm). The performance analysis was performed by checking the speed, torque and power, the values of each of them were reported on the dynamometer control panel. Fuel consumption was determined by measuring the change in fuel mass over a period. Engine speed during the tests was varied due to the increased load imposed by the dynamometer. The engine performance parameters were obtained for 8 different speeds, 2750, 2600, 2450, 2300, 2150, 2000, 1850 and 1700 rpm. The engine was tested for two compression ratios, that is, for 20:1 and 21.5:1, and for two start of injection, i.e., 10° and 17°BTDC. Therefore, the tests were named by: CR20-SOI10; CR20-SOI17; CR21.5-SOI10; and CR21.5-SOI17, respectively. When operating with HET-OM blends the engine followed the evaluation steps described above, where the analyses were carried out with the two blends defined.

3. RESULTS AND DISCUSSION

The evaluation of the fuel viscosity was carried out with a measurement range of 30 °C to 70 °C and the results obtained for the different fuels are reported in the Table 3. The specific mass of fuels obtained at 20 ºC are shown in table 4, with the HET70OM30 blend showing the smallest variation in relation to DO, i.e., 1.6%. Using equations (3) and (4), Table 5 shows the *LHV* values of the fuels.

Apparently, the HET-OM mixtures showed total miscibility. The densities of the mixtures were greater than the density of the DO, since the presence of OM in the mixture tends to increase its value. The HET70OM30 mixture tended to be closer to the DO density with a variation of 1.6%, thanks to the greater proportion of HET. The viscosity varied according to the temperature of the fluid, with the tendency of HET in the mixtures to evaporate as the temperature increases. This was detected by increasing the viscosity of the mixtures at higher temperatures. However, at ambient temperatures, the evaporation of HET does not significantly influence the results, where the mixture HET60OM40 had a viscosity about 24.2% higher than that of DO100 and the mixture HET70OM30, 17.8% lower due to the higher concentration of HET. According to Table 5, ethanol has the lowest LHV of the evaluated fuels, and when mixed with OM, the heating value increases in relation to the result of HET, however, it is below the value of the LHV of OM. Thus, because HET and OM have an LHV lower than DO, HET-OM mixtures also have a lower LHV than DO, being 32.6% lower for HET60OM40 and 35.3% lower for HET70OM30.

Table 3. Viscosity of the fuel samples versus temperature

Fuel	Viscosity [cP]								
	30 °C	35 °C	40 °C	45 °C	50 °C	55 °C	60 °C	65 °C	70 °C
OM100	366.8	264.8	197.0	146.9	111.9	87.5	68.6	55.7	46.2
DO100	2.6	2.4	2.2	2.1	2.0	1.9	1.8	1.7	1.6
HET60OM40	3.3	2.6	-	-	-	-	-	-	-
HET70OM30	2.2	1.8	1.4	1.0	0.7	0.6	-	-	-

Table 4. Specific mass of the fuel samples

Fuel	Density [kg/L]
OM100	0.955
HET100	0.810
DO100	0.843
HET60OM40	0.871
HET70OM30	0.857

Table 5. Lower Heating Value of the fuel samples

Blend	Fuel	Volume [mL]	Mass [g]	Mass fraction	*LHV* [kJ/kg]
-	DO	-	-	-	42653
-	HET	-	-	-	23924
-	OM	-	-	-	34903
HET60-OM40	HET	11250	9112.5	0.560	28755
	OM	7500	7162.5	0.440	
HET70-OM30	HET	12800	10368	0.664	27613
	OM	5500	5252.5	0.336	

The power is obtained by multiplying the torque by rotation; thus, power curves tend to behave similarly to the torque curves. Figures 2 and 3 show the power curves obtained in the experiments, being evidenced for some HET-OM power curves a discontinuity due to irregular engine operation. In these figures are also showed the error bars. The power results presented in the following curves refer to the values measured in the dynamometric tests. In general, it is noted that the greatest power developed by engine with the different settings of adjustment, CR and SOI, was to DO operation. The mixtures of fuels evaluated, HET60OM40 and HET70OM30, presented adverse power results, tending to approximate the DO results in some rotations, but in others, they present great variations. The blends showed varied results, however, in most evaluations the power also tended to present higher values at higher speeds.

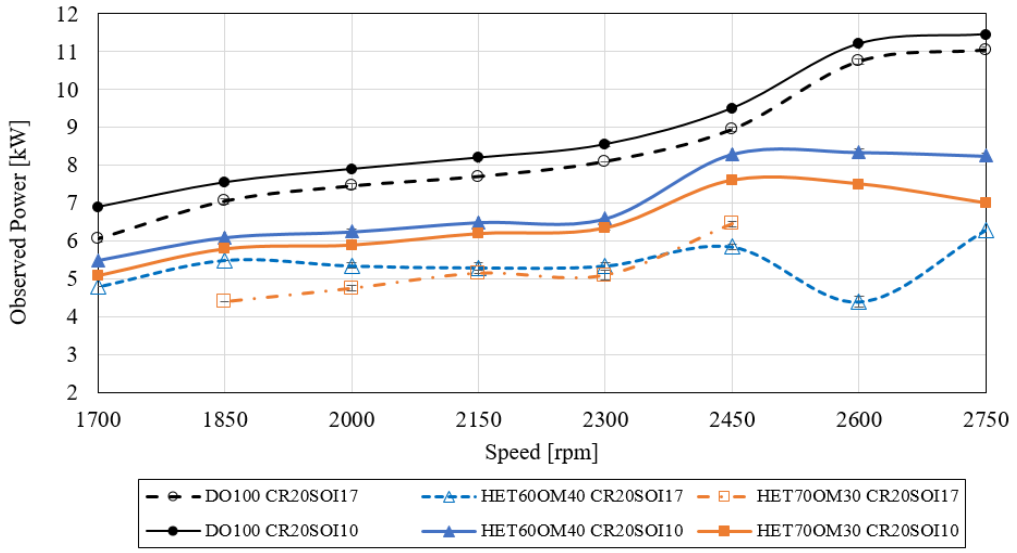

Figure 2. Observed power for CR20-SOI10 and CR20-SOI17 samples

The DO power curve has an upward ramp characteristic from low speed to 2750 rpm of maximum power. The characteristic curves for HET-OM mixtures have an approximately planar behavior. The configuration that showed the greatest operational stability with HET-OM mixtures was CR21.5-SOI17. In this engine configuration it was achivied the highest power. The maximum power obtained was to DO operation, which was about 12.8 kW, for the CR of 21.5:1 and SOI of 17° at the rotation of 2750 rpm. In the same engine configuration, the HET60OM40 mixture had a maximum power of 5.2 kW at 1700 rpm and the HET70OM30 mixture of 4.1 kW at 1850 rpm. The HET-OM blends showed power results with low variation trends, but the results were smaller than those for DO.

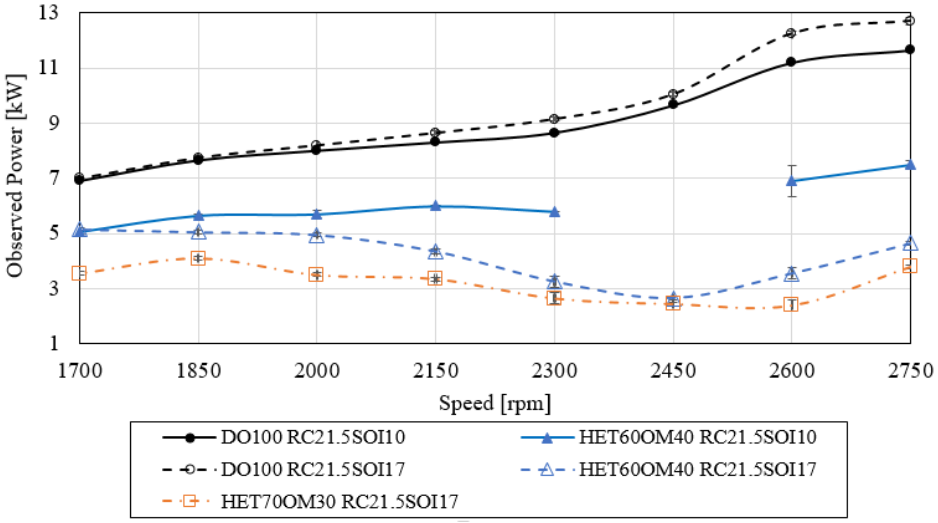

Figure 3. Observed power for CR21.5-SOI10 and CR21.5- SOI17 samples

In Table 6 are reported the results of observed specific fuel consumption for diesel fuel and for the best results for the HET-OM analysed, which was at HET60-OM40 blend. According to Table 6 it is possible to observe that the fuel consumption for the blend HET60-OM40 was higher than DO100 for all engine configuration tested. The highest specific fuel consumption found for HET60-OM40 was 566 g/kWh for CR21.5-SOI17 at 2450 rpm, while the highest consumption for DO100 operation was 327.4 g/kWh for CR20-SOI10 at 1700 rpm. The higher specific fuel consumption for HET60-OM40 can be explained by the lower heating value of the mixture, which was 28755 kJ/kg compared to 42653 kJ/kg to DO100, so more amount of fuel is necessary to deliver the same amount of energy.

Table 6. Observed specific fuel consumption [g/kWh]

Speed [rpm]	Condition							
	CR20-SOI10		CR20-SOI17		CR21.5-SOI10		CR21.5-SOI17	
	DO100	HET60-OM40	DO100	HET60-OM40	DO100	HET60-OM40	DO100	HET60-OM40
2750	269.0	347.1	249.5	333.8	238.3	343.4	239.9	427.4
2600	270.4	351.9	256.0	453.4	258.2	419.8	216.6	489.3
2450	271.0	372.3	285.6	378.6	317.9	-	269.1	566.0
2300	318.5	433.6	308.1	421.8	278.8	427.8	302.0	487.9
2150	327.9	443.8	306.6	407.9	274.4	408.5	279.2	431.9
2000	335.2	386.4	287.5	404.8	300.6	447.6	296.3	392.1
1850	282.4	352.1	293.5	378.7	290.6	402.5	309.8	366.0
1700	327.4	442.9	293.1	387.9	321.1	402.7	289.0	408.7

Fuel conversion efficiency was calculated using Eq. (2) and Figure 4 illustrates the η_f results for DO100 and HET60-OM40 operation. In general, the fuel conversion efficiencies were higher for HET60-OM40, especially at low speeds. The highest fuel conversion efficiency achieved for HET60-OM40 blend was 37.5% for CR20-SOI17, representing an improvement about 11% in relation to DO operation. However, for higher compression ratio and start of injection at 2450 and 2600 rpm the fuel conversion efficiency for HET60-OM40 was deteriorated. At 2600 rpm and CR21.5-SOI17, the conversion efficiency was 25.6% for HET60-OM40, while DO100 achivied the highest fuel conversion efficiency of 39%. One reason for the improvement in the fuel conversion efficiency can atrribuited to the reduction in the exhaust gas temperature (EGT) of HET-OM blend in relation to those obtained with DO, as is shown in Figure 5. The reduction in EGT is related to the presence of HET in the mixtures, which contributes to the reduction of the temperature in the combustion chamber due to its high latent heat of vaporization (KUMAR et al., 2013). In this regard, the lower exhaust gas temperature result in a reduction of the heat losses and, consequently, increasing fuel conversion efficiency.

The smoke opacity is an indirect parameter of soot and particulate matter content in the exhaust gases. Figure 6 exhibits the behavior of smoke index with different engine speeds, compression ratio, and start of injection for DO100 and HET60-OM40 operation. The smoke opacity for DO100 operation varied from 5 to 7.5% and it is possible to observe that opacity for DO100 operation decreased for start of injection of 17° and compression ratio of 21.5. However, when the engine operated with HET60OM40 the opacity decreased significantly, to the point of being “zero” in more than one evaluated speed. The highest smoke opacity found for HET60-OM40 was 0.45%, representing a

reduction about 92.5% in relation to DO operation in the same speed and engine configuration. The reduction in the smoke opacity is attributed to the fact that HET and OM have more oxygen in its composition and also because they have lower amounts of carbon in its molecule in relation to diesel fuel. Therefore, when more HET and OM is used less carbon is burned, resulting in a reduction in smoke opacity.

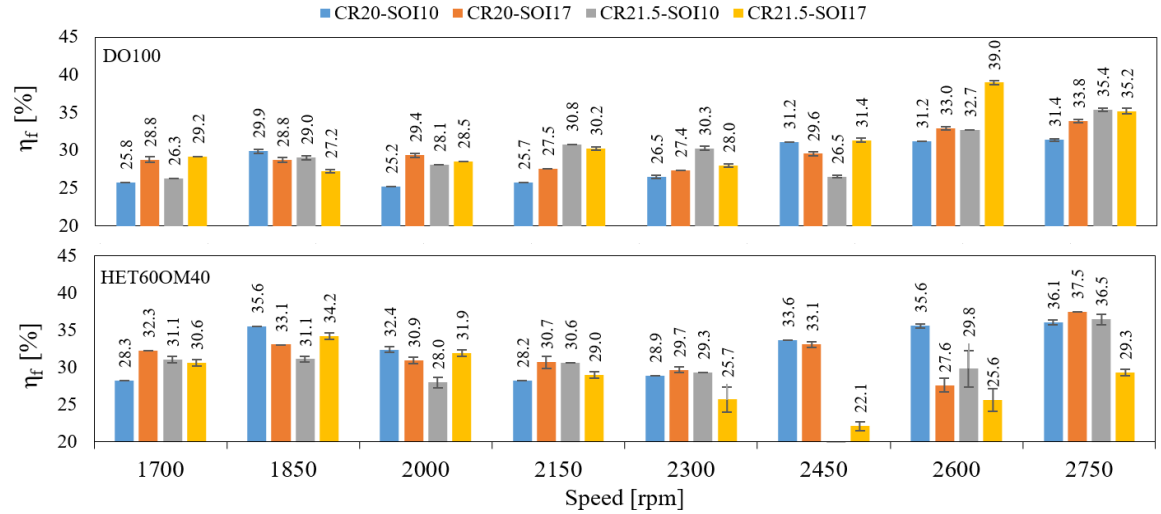

Figure 4. Fuel conversion efficiency

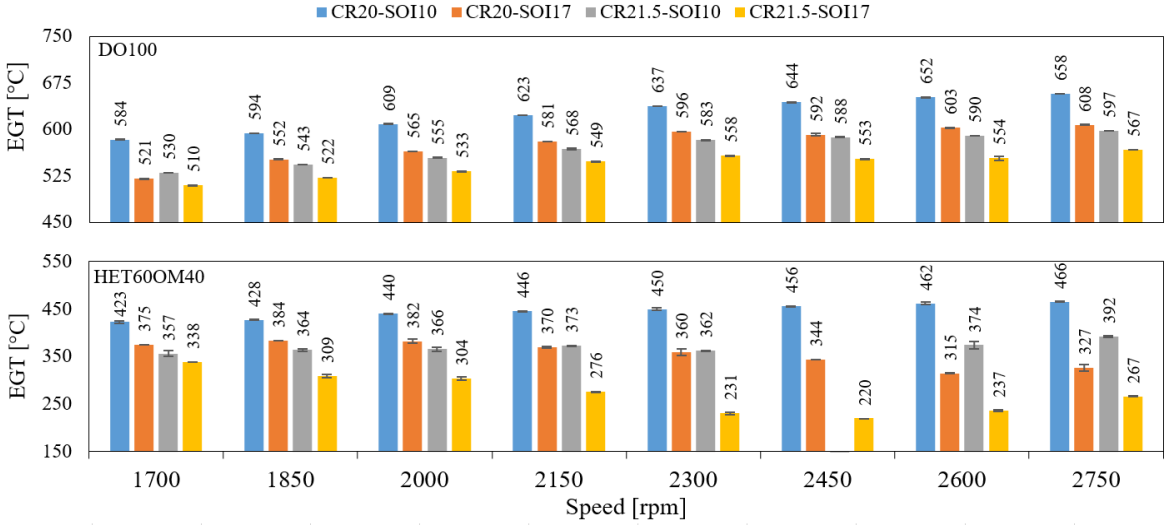

Figure 5. Exhaust gas temperature (EGT)

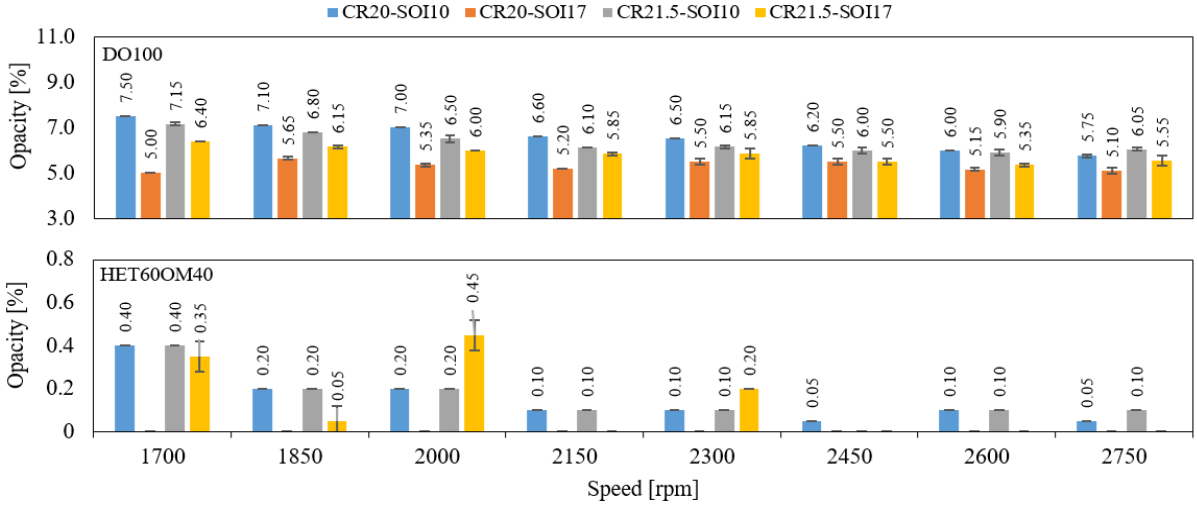

Figure 6. Smoke opacity

Figure 7 shows the CO emission results obtained for the D100 and HET60-OM40 blend. It is noted that when the engine speed and start of injection increase, the CO emissions tend to decrease for the diesel fuel operation. The results indicated a meaningfully reduction of CO emissions when the engine operated with HET60-OM40 blend in relation to DO100 operation. In DO100 operation, the CO emissions ranged from 0.32 to 1.19% in volume, while the highest value for HET60-OM40 operation was 0.13% and the lowest 0.02% in volume. On average, the use of the HET60OM40 mixture instead of diesel fuel reduced CO emissions by around 90.3%.

The same trend of results for CO emissions can be observed for CO_2 emissions, as can be seen in Figure 8. Diesel fuel operation resulted in CO_2 emissions between 10.5 to 11.6%.When the engine operated with the biofuel mixture, CO_2 emissions drastically reduced, varying from 3.9 to 8.3% in volume.

The reduction of CO and CO_2 emissions when the engine operated with HET60OM40 is due to the less carbon and higher oxygen in chemical composition of ethanol and castor oil. In this regard, when the engine operated with this biofuel mixture, less carbon was available inside the cylinder, which reduces CO and CO_2 production.

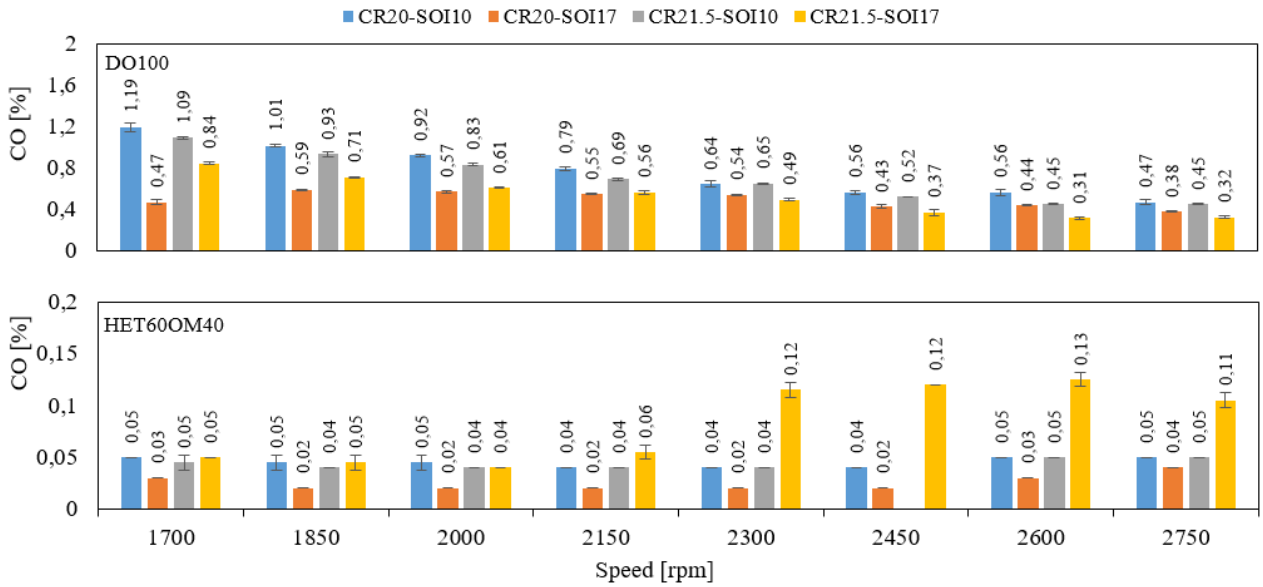

Figure 7. CO emissions

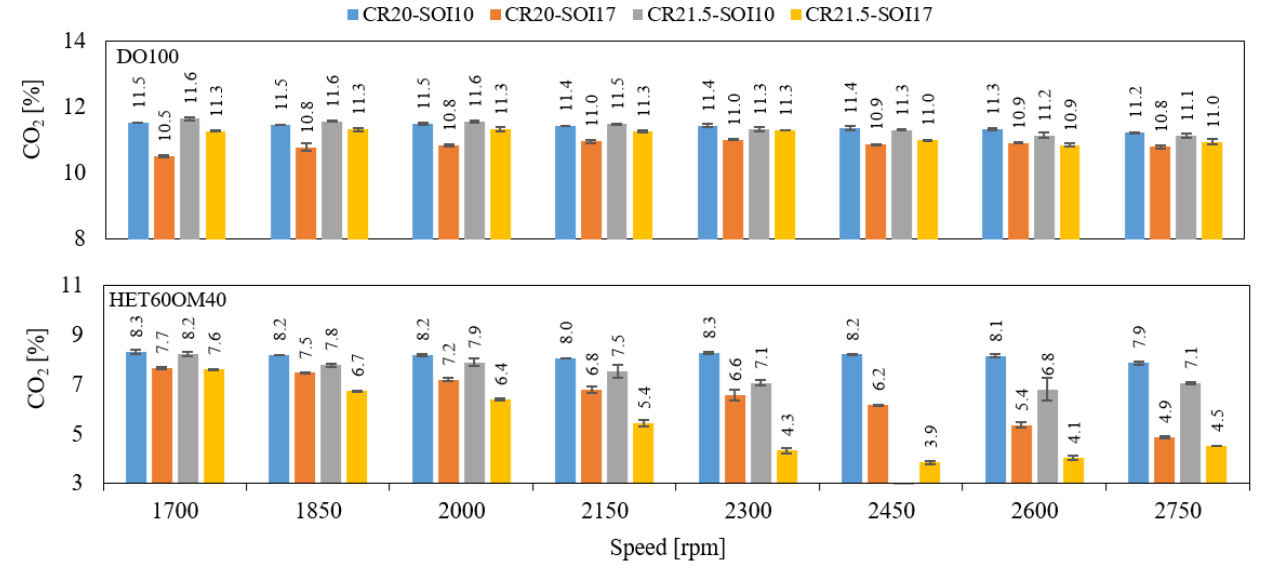

Figure 8. CO_2 emissions

The results of the hydrocarbon emissions (HC) are shown on Figure 9. The HC emissions increase as the engine operates with the HET60OM40. In DO100 operation, the HC emissions were higher for CR20-SOI17 and CR21.5-SOI17 engine configuration, varying from 14 to 37 ppm, while for CR20-SOI10 and CR21.5-SOI10 ranged from 7 to 9 ppm. Figure 9 shows a considerably increase in hydrocarbons emissions when the engine operates with HET60OM40. The lowest values of HC emissions found was 78 ppm in volume for HET60OM4 at CR20-SOI10, 1700 and 1850 rpm.

However, for this same engine speed was found the highest HC emissions, reaching the values of 181 ppm for 1700 rpm and 138 ppm for 1850 rpm.

The expressive increase in HC emissions is justified because ethanol has a cooling effect in the combustion process due to the higher latent heat of vaporization. As a result, the low combustion temperature may not be able to ignite all the charge and not burn all fuel during the expansion stroke, which was evidenced in some tests by the detection of liquid fuel in the exhaust line, which leads to increased HC emission. The results found coincide with the literature of Prakash et al., 2018.

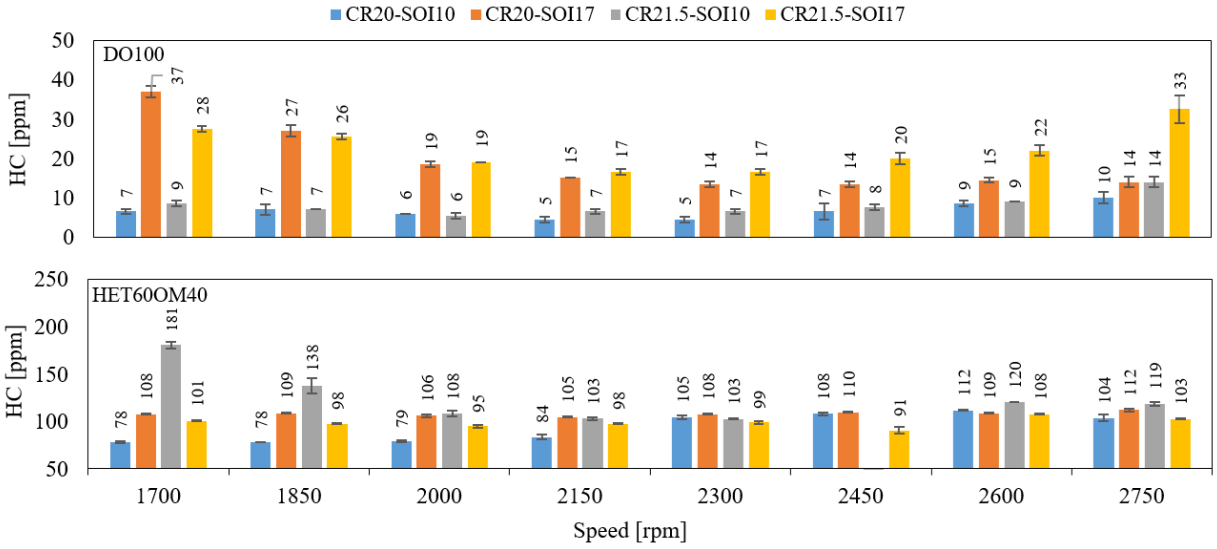

Figure 9. HC emissions

Figure 10 illustrates the NO_X emissions for diesel fuel and ethanol-castor oil blend. NO_X emissions were lower when the engine operated with HET-OM blends, to the point that no speed evaluated have higher emissions than DO. In general, it is clear that for CR20-SOI17 and CR21.5-SOI7 configurations the NO_X emissions was higher than others configurations, except for the HET60-OM40 at higher engine speeds. For diesel fuel operation, NO_X emissions ranged from 449 to 1160 ppm in volume, while for HET60-OM40 the NO_X decreased from 751 ppm to 63. Maximum reduction in NO_X observed was 94% at CR21.5-SOI17 and 2600 rpm, resulting in 63 ppm for HET-OM blend compared to the 1065 ppm for DO100 operation. The average reduction in NO_X emissions was about 58% with the engine operating in biofuel mode. The main reason for this reduction is due to the lower temperature in the combustion chamber caused by the high ethanol latent heat of vaporization, which can be evidenced indirectly by the exhaust gas temperature measurements, which results in the reduction of NO_X formation.

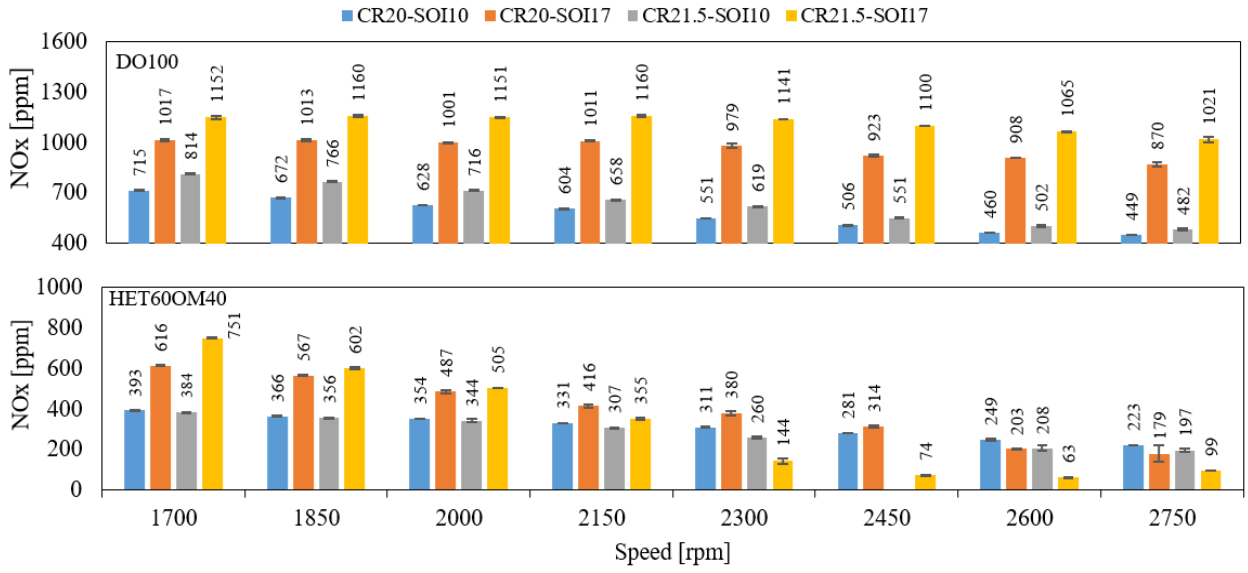

Figure 10. NO_X emissions

4. CONCLUSION

In general, the emission results obtained were satisfactory, where HET-OM blend showed significant emissions reductions of CO, CO_2, smoke opacity and NO_X. In addition, the fuel conversion efficiencies results were also satisfactory, being, in general higher, than pure diesel fuel operation. The maximum fuel conversion efficiency achieved for HET-OM blend was 37.5% at CR20-SOI17 and 2750 rpm. On the other hand, hydrocarbon emission demonstrated a great increase, reaching the value of 181 ppm at low speed, although with the increase in engine speed the average was 115 ppm. Moreover, the specific fuel consumption also increased when the engine operated with HET-OM blend in relation to DO operation.

The future forecast for the automotive sector, for products that use internal combustion engines, is to meet increasingly lower levels of emissions. Thus, in addition to management and control systems for vehicle exhaust gases developed by automakers and manufacturers, the development of fuels, which when burned generate less pollutant emissions, is a fundamental need to comply with legislation. This will greatly contribute to the overall preservation of the planet, corroborating the possibility of total substitution of petroleum-based fuels.

5. ACKNOWLEDGEMENTS

G. D. Telli thanks CNPq (Brazilian National Council for Scientific and Technological Development) for the doctorate scholarship.

6. REFERENCES

Brunelli, R. R. 2009. *Estudo de viabilidade operacional e desempenho de motores de combustão interna operando com combustível biodiesel em relação ao combustível diesel automotivo*. 2009. 159 f. Dissertação (mestrado) – Curso de Engenharia Mecânica, Universidade Federal do Rio Grande do Sul, Porto Alegre.

International Energy Agency. 2018. Renewables 2018 analysis and forecasts to 2023. Executive Summary., p. 5.

Kumar, S.; Cho, J. H.; Park, J.; Moon, I., 2013. Advances in diesel-alcohol blends and their effects on the performance and emissions of diesel engines. *Renewable and Sustainable Energy Reviews*, Vol. 22, pp. 46–72.

Pinzi, S.; López, I.; Leiva-Candia, D. E.; Redel-Macías, M. D.; Herreros, J. M.; Cubero-Atienza, A.; Dorado, M. P., 2018. Castor oil enhanced effect on fuel ethanol-diesel fuel blends properties. *Applied Energy*, Vol. 224, pp. 409-416.

Prakash, T.; Geo, V. E.; Martin, L. J.; Nagalingam, B., 2018. Effect of ternary blends of bio-ethanol, diesel and castor oil on performance, emission and combustion in a CI engine. *Renewable Energy*, Vol. 122, pp. 301-309.

Telli, G.D., Altafini, C.R., Rosa, J.S., and Costa, C.A., 2018a. "Experimental analysis of a small engine operating on diesel–natural gas and soybean vegetable oil–natural gas". *Journal of the Brazilian Society of Mechanical Sciences and Engineering*, 40:547.

Vailatti, M.A., Altafini, C.R., Telli, G.D. and Rosa, J.S., 2017. "Experimental analysis of a small generator set operating on dual fuel diesel-ethanol". *Scientia cum Industria*. Vol. 5, No. 1, pp. 1-9.

6. RESPONSIBILITY NOTICE

The author(s) is (are) the only responsible for the printed material included in this paper.